Struct Multidisc Optim 23, 49–62 © Springer-Verlag 2001

Topology optimization of compliant mechanisms with multiple materials using a peak function material interpolation scheme

L. Yin and G.K. Ananthasuresh

Abstract In the topology optimization of structures, compliant mechanisms or materials, a density-like function is often used for material interpolation to overcome the computational difficulties encountered in the large "0-1" type integer programming problem. In this paper, we illustrate that a gradually formed continuous peak function can be used for material interpolation. One of the advantages of introducing the peak function is that multiple materials can easily be incorporated into the topology optimization without increasing the number of design variables. By using the peak function and the optimality criteria method, we synthesize compliant mechanisms with multiple materials with and without the material resource constraint. The numerical examples include the two-phase, three-phase, and four-phase materials where *void* is treated as one material. This new design method enables us to optimally juxtapose stiff and flexible materials in compliant mechanisms, which can be built using modern manufacturing methods.

Key words material interpolation, topology optimization, optimality criteria, compliant mechanism, heterogeneous material

1 Introduction

The topology optimization of continuum structures, compliant mechanisms, or materials tries to optimally distribute material in a fixed reference domain. Employing a material interpolation function, the finite element method for the fixed reference domain, and an optimization algorithm has been proven to be very successful in determining optimum continuum topologies (Bendsøe 1995). There are several key issues in this method. They include: (i) a well-posed objective function, (ii) appropriate constraints, (iii) appropriate material interpolation function, and (iv) an efficient optimization algorithm. Many objective functions and appropriate constraints are suggested for various problems in the literature such as stiff structures (Bendsøe and Kikuchi 1988), vibrating structures (Ma and Kikuchi 1995), compliant mechanisms (Ananthasuresh *et al.* 1994a,b), material design (Sigmund 1994), tunnel support (Yin *et al.* 2000; Yin and Yang 2000a,b), prevention of crack propagation (Yin and Yang 2000c), etc. However, the other two problems, which are fundamental and encountered in every application, are still argued in the literature.

In many applications, we expect the optimal topology of a structure to consist solely of one material and void. This necessitates a "0-1" type integer parametrization of the design domain to decide if material should be placed at a point or not. Obtaining reasonable solutions of the "0-1" type large-scale integer programming problem is a computationally daunting task. Along the idea of the *homogenization method* (Bendsøe and Kikuchi 1988) to relax the "0-1" problem, many methods are suggested to overcome the computational difficulties of the integer-programming problem by treating the reference domain as if it is made of a composite material consisting a solid and void and varying its microstructure. A majority of these methods use density-like material interpolating functions that continuously vary between 0 and 1. For such density-like functions, a question often arises as to whether a corresponding material microstructure physically exists. This is a concern especially if intermediate gray-scale densities prevail in the final solution. This is not a concern in the original homogenization method of Bendsøe and Kikuchi (1988) because it is based on the microstructure variation of a composite material consisting of a material and an oriented void. On the other hand, the widely used density-like function called SIMP (Solid Isotropic Material with Penalization) model (e.g. Rozvany *et al.* 1995; Zhou and Rozvany 1991) is originally not intended to correspond to a physical microstructure (Bendsøe 1989). However, recently Bendsøe and Sigmund (2000) concluded that there exist physical microstructures for SIMP functions for a suitably chosen exponent

Received July 20, 2000
Revised manuscript received September 29, 2000

L. Yin and G.K. Ananthasuresh

Department of Mechanical Engineering and Applied Mechanics, University of Pennsylvania, Philadelphia, PA 19104, USA
e-mail: {luzhongy,gksuresh}@seas.upenn.edu

η in the following material interpolation function where ρ denotes the material "density":

$$\mathbf{E}_{ijk\ell} = \rho^{\eta}\mathbf{E}^{0}_{ijk\ell}\,. \tag{1}$$

They noted that when η is greater than or equal to three, the SIMP model obeys Hashin and Shtrikman (1963) bounds on the effective properties of composite materials, and therefore bears out physical microstructure. However, since the original problem is a "0-1" type delta function, it will be interesting to explore more direct ways of interpolating the material between zero and one. There indeed exist many continuous functions that approximate the delta function. In this paper we employ one such function, which we call a *peak function* for brevity, and show that it not only works well but also provides some advantages over previously used material interpolation functions. One of the principal advantages is the ability to include multiple materials without increasing the number of design variables in the optimization procedure. A resource constraint on the amount of available material can also be easily included.

By taking advantage of the peak function to interpolate the material, we formulate a new problem for compliant mechanisms that are comprised of stiff and flexible materials in a monolithic structure. We also present an iterative update scheme to solve this problem using the optimality criteria method. One of the motivations for the multimaterial compliant mechanism design problem is the availability of modern manufacturing methods such as the shape deposition manufacturing (Rajagopalan *et al.* 2000), layered manufacturing with embedded components (Bailey *et al.* 2000), co-extrusion of plastics, etc. These methods are capable of economical manufacture of three-phase material designs where void is considered as one phase.

2
Compliant mechanisms

Compliant mechanisms are elastic continua that are designed to be sufficiently flexible to deform and act like rigid-link mechanisms. They have many advantages as described in the recent literature on this subject. Compliance in these mechanisms can exist either in the lumped form as flexural pivots (the so-called *living hinges*) or in the distributed form where the whole structure deforms to varying degree. Both kinematics-based (Howell and Midha 1996; Mettlach and Midha 1996; Saxena and Kramer 1998); and continuum mechanics-based (e.g. Ananthasuresh *et al.* 1994a; Sigmund 1997; Frecker *et al.* 1997; Nishiwaki *et al.* 1998; Hetrick and Kota 1998; Saxena and Ananthasuresh 2000) design methods have been developed for compliant mechanisms. In the continuum mechanics-based methods, the material is optimally distributed in a fixed design domain to define a topology. In the solutions obtained using such methods, it is not uncommon to see the semblance of flexural pivots and relatively rigid segments within the monolithic object. An example of this is shown in Fig. 1.

Fig. 1 Appearance of flexural pivots in continuum compliant topologies. (a) Problem specifications, (b) optimized topology

The most general compliant mechanism can consist of compliant and or rigid segments joined with compliant and/or rigid (i.e. kinematics) joints excluding the special case of all rigid segments and joints. Hence, a question arises as to what is the optimal balance between rigidity and compliance for a given set of problem specifications. This question can be partially answered by considering a two-material model where one material is much more flexible (lower Young's modulus) than the other. The second motivation is the need to design compliant mechanisms to be flexible and strong. Using two or more materials, it is possible to obtain large deformations without exceeding the strengths of the materials. The third motivation for pursuing two-material compliant mechanism design is the emergence of manufacturing methods that are capable of producing heterogeneous parts without assembly and with strong inter-material interfaces. New design methods are necessary to take full advantage of such techniques. The fourth motivation is to mimic Nature's compliant designs that are usually made up of rigid and flexible materials (Vogel 1995; Full 1997).

3
Problem statement

In the spirit of topology optimization methods for compliant mechanisms, we seek optimal material distribution in a fixed reference domain so that the mechanism can most efficiently resist the external forces and at the same time it can produce maximum displacement at the output port. We suppose that the optimal mechanism consists of $(n+1)$ material phases. The $(n+1)$-st phase refers to the void (i.e. no material) in order to define holes in the topology of the optimal continuum. The m-th phase material occupies a domain Ω^m, which is a part of the fixed reference design domain Ω. The external forces and displacement boundary conditions are given on the fixed design domain, as shown in Fig. 2. The problem we consider here is linearly elastic in 2-D space although further generalizations are not precluded. Figure 2a shows an input force F at the input port Γ_{in}, and an expected output displace-

ment Δ_{out} at output port Γ_{out}. We may require that the output port resist an output force when interacting with its surroundings. Following the work of Ananthasuresh *et al.* (1994a), we use a linear spring of spring constant k_s at the output port to model the work-piece that is being acted upon. To facilitate analytical formulation, we consider another load condition for the mechanism as shown in Fig. 2b, which is a unit dummy force f that acts at the output port Γ_{out} in the direction of the output displacement. Then, the output displacement Δ_{out} can be expressed in the form of the *mutual strain energy* as

$$\Delta_{\text{out}} = \int_{\Omega} \epsilon(u) : E : \epsilon(v)\, \mathrm{d}\Omega = \int_{\Gamma_{\text{in}}} F \cdot v\, \mathrm{d}\Gamma. \tag{2}$$

u is the equilibrium displacement field under the input force F, v is the equilibrium displacement field under the unit dummy force f.

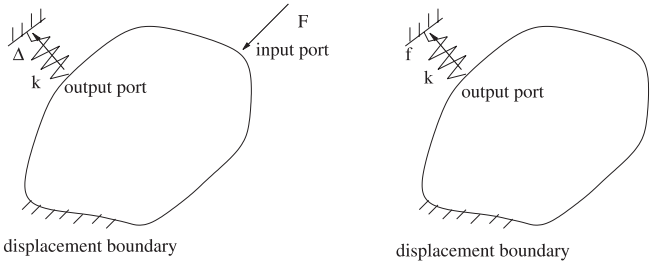

Fig. 2 Problem definition

Based on previous formulations (Saxena and Ananthasuresh 2000) and using the two load conditions of the mechanism, the design problem can be stated as

$$\text{minimize} \left[-\frac{\int_{\Omega} \epsilon(u) : E : \epsilon(v)\, \mathrm{d}\Omega}{\int_{\Omega} \epsilon(u) : E : \epsilon(u)\, \mathrm{d}\Omega} = -\frac{\int_{\Gamma_{\text{in}}} F \cdot v\, \mathrm{d}\Gamma}{\int_{\Gamma_{\text{in}}} F \cdot u\, \mathrm{d}\Gamma} \right] \tag{3}$$

subject to

$$\int_{\Omega} \epsilon(u) : E : \epsilon(w_u)\, \mathrm{d}\Omega = \int_{\Gamma_{\text{in}}} F \cdot w_u\, \mathrm{d}\Gamma \quad \text{for all } w_u \in U\,, \tag{4}$$

$$\int_{\Omega} \epsilon(v) : E : \epsilon(w_v)\, \mathrm{d}\Omega = \int_{\Gamma_{\text{out}}} f \cdot w_v\, \mathrm{d}\Gamma \quad \text{for all } w_v \in U\,, \tag{5}$$

$$\mathbf{E}_{ijkl}(x) = \sum_{m=1}^{n} \delta_m(x) \mathbf{E}^m_{ijkl}\,, \tag{6}$$

$$\delta_m(x) = \begin{cases} 1 & \text{if } x \in \Omega^m \\ 0 & \text{if } x \in \Omega / \Omega^m \end{cases}. \tag{7}$$

Here, the minimized entity in (3) is a multicriteria objective function that reflects maximizing the ratio of flexibility and stiffness measures, and (4) and (5) are the equilibrium equations for the two load conditions shown in Fig. 2. They are cast into their weak, variational form, with U denoting the space of kinematically admissible displacement field, and ϵ linearized strain tensor. In (6), $\mathbf{E}^m_{ijkl}$ denotes the constitutive linear material property tensor of the m-th elastic material from which the mechanism is to be formed. The function $\delta_m(x)$ is a point-wise function denoting where the m-th phase material exists. Its value should be zero or one in the optimized design in order to be manufactured easily. The peak function material interpolation model that meets this requirement is presented next.

4
Peak function material interpolation model

The optimization problem stated in (3) is a discrete optimization problem that is difficult to solve. Thus, relaxed formulations are commonly used in the literature. Two relaxed formulations are popularly used. One is the homogenization method and the other is the SIMP method. These two and others view the material distribution problem as a variable microstructural or artificial density allocation problem. In the SIMP method, such a density is expressed as shown below for a two-phase material where void is one "material",

$$\mathbf{E}_{ijk\ell} = \rho^{\eta} \mathbf{E}^0_{ijk\ell}\,, \tag{8}$$

where $\mathbf{E}_{ijk\ell}$ is the relaxed tensor of material properties in the design domain, ρ the density of the material $\mathbf{E}^0_{ijk\ell}$, with the parameter η to penalize the intermediate densities in the final solution. For the three-phase material design the SIMP formulation gives

$$\mathbf{E}_{ijk\ell} = \rho_1^{\eta_1} \left(\rho_2^{\eta_2} \mathbf{E}^1_{ijk\ell} + (1 - \rho_2^{\eta_2}) \mathbf{E}^2_{ijk\ell} \right), \tag{9}$$

where the density of material $\mathbf{E}^1_{ijk\ell}$ is $\rho_1 \rho_2$ and the density of material $\mathbf{E}^2_{ijk\ell}$ is $\rho_1 (1 - \rho_2)$, with the penalty parameters η_1 and η_2. Thus, the number of design variables ρ_i is doubled in the three-phase material model compared to the two-phase material model. For more than three phases of materials, the interpolation model in the SIMP method becomes even more complicated. We present an alternative material interpolation model that does not increase the number of design variables as the number of material phases increases. According to (6) and (7), we can see that in the material model the function δ_m is ideally a δ function. As noted before, a continuous function is needed for the numerical optimization. Such a function need not correspond to a physical microstructure of a material nor be viewed as a density of the material provided that the final solution approaches the δ function model. A number of smooth functions that approximate the δ function exist (Arfken 1970). We consider

here the normal distribution function to interpolate the material properties of multimaterial continuum.

The normal distribution function is given as

$$\exp\left[-\frac{(\rho-\mu_m)^2}{2\sigma_m^2}\right],$$

where ρ is the variable parameter with mean μ_m and standard deviation σ_m. Using this function, (6) can be rewritten as a *peak function* material interpolation model given by

$$\mathbf{E}_{ijk\ell} = \sum_{m=1}^{n} \mathbf{E}^m_{ijk\ell} \exp\left[-\frac{(\rho-\mu_m)^2}{2\sigma_m^2}\right] + \mathbf{E}^{\text{void}}_{ijk\ell}, \tag{10}$$

with ρ as the relaxed continuous design variable. With small enough σ_m, the function $\exp\left[-\frac{(\mu-\mu_m)^2}{2\sigma_m^2}\right]$ is a continuous approximation to δ-function. That is, if at some space point $\mathbf{x}$ where ρ is equal to μ_m there will exist m^{th} phase material exclusively. Likewise, when all σ_m's are sufficiently small so that peaks are created at the corresponding μ_m's, a value of ρ that is different from μ_m's gives rise to a void. The tensor $\mathbf{E}^{void}_{ijk\ell}$ is chosen to be very small, but not zero, to avoid numerical problems in the finite element analysis. Thus, by appropriately choosing μ_m for each phase, a single variable ρ can be used to select among multiple materials and void. For example for a two-phase material model, (10) becomes

$$\mathbf{E}_{ijk\ell} = \mathbf{E}^1_{ijk\ell} \exp\left[-\frac{(\rho-\mu_1)^2}{2\sigma_1^2}\right] + \mathbf{E}^{\text{void}}_{ijk\ell} \tag{11}$$

and for a three-phase material model,

$$\mathbf{E}_{ijk\ell} = \mathbf{E}^1_{ijk\ell} \exp\left[-\frac{(\rho-\mu_1)^2}{2\sigma_1^2}\right] +$$

$$\mathbf{E}^2_{ijk\ell} \exp\left[-\frac{(\rho-\mu_2)^2}{2\sigma_2^2}\right] + \mathbf{E}^{\text{void}}_{ijk\ell}. \tag{12}$$

It is just as easy to write down the four or higher phase material model according to (10).

An additional advantage of the peak function model is that the design variable is free to take any value between $-\infty$ to ∞ and hence side constraints on the bounds on the design variables are not necessary in the optimization problem. Furthermore, it is worth noting that the material interpolation model in (10) intrinsically has both the upper and lower bounds irrespective of the variable ρ.

For more than two phases of material, the interpolation model of (10) poses some difficulty in the numerical procedure. We take the three-phase material design as an example to illustrate the difficulty and how to overcome it. In (12), we take the two materials as isotropic with Young's modulus for the first phase 100 and the second phase 10, $\sigma_1 = \sigma_2 = 0.05$, $\mu_1 = 0$, and $\mu_2 = 0.3$. The relationship between ρ and Young's modulus E are shown in Fig. 3a. It can be seen in this figure that there exists a point with zero slope on the curve between $\mu = 0$ and $\mu = 0.3$. This zero slope is a potential source of difficulty in the numerical calculations. Since all steps for searching optimal value of ρ depend on the slope of the local point on the curve, the algorithm may have difficulty to cross this point to make transition from one material phase to the other during the optimization process. In such a case, the initial guess would strongly influence which material phase exists in any given portion of the reference design domain. For instance, if the initial value for ρ is taken as 0.25, the final design might consist only of the second phase material and the void. Similarly, if the initial value for ρ taken as 0.1, the final design might consist of the first phase material and the void. To get a reasonable transition between the material phases, we begin with large values of σ_m $(m = 1, \ldots, n)$ in (12), and then gradually decrease the values after each iteration in the optimization procedure until we get a very close approximation to the δ-function. That is,

$$\sigma_m^{(k+1)2} = \sigma_m^{(k)2}(1-\omega) \quad \text{for } m = 1, \ldots, n, \tag{13}$$

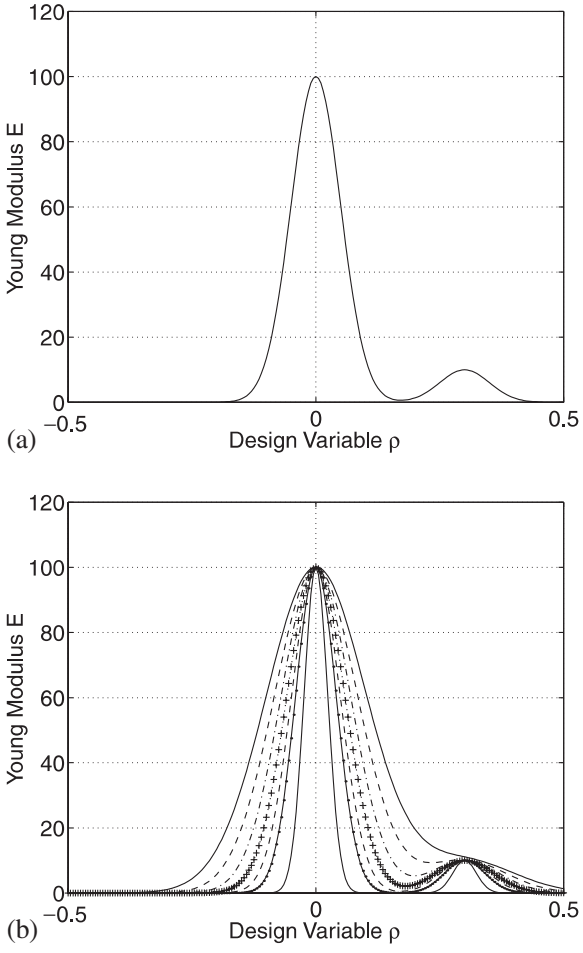

Fig. 3 Gradual tightening of the relaxed three-phase material interpolation model

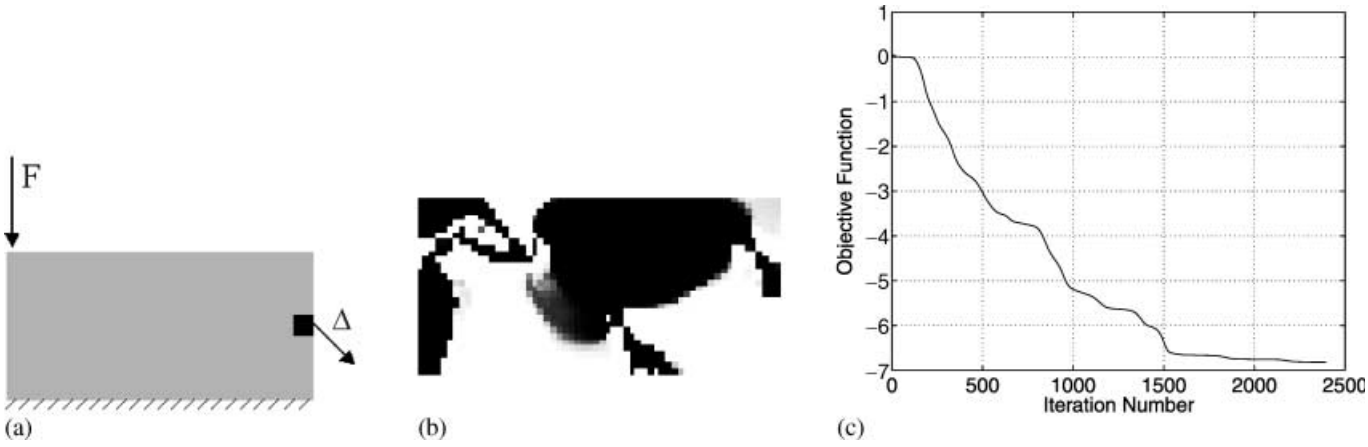

Fig. 4 A two-phase material compliant mechanism. (a) Specifications, (b) optimal topology, (c) convergence history

where the superscripts (k) and $(k+1)$ denote the k-th and $(k+1)$-st iterations, and ω is the rate at which σ_m^2's are decreased. This is pictorially illustrated in Fig. 3b. By incorporating this into the optimization procedure, we can get reasonable transition and separation between different material phases. This is demonstrated in the examples presented in Sect. 6.

4.1
Material resource constraint

A material resource constraint (i.e. the volume constraint) can easily be included using the peak function interpolation model. As shown in the inequality below, one design variable ρ is sufficient to pose a very general constraint,

$$\int_{\Omega} \sum_{m=1}^{n} w_m \exp\left[-\frac{(\rho-\mu_m)^2}{2\sigma_m^2}\right] \mathrm{d}\Omega \le V^* \,, \tag{14}$$

where $w_m (m = 1, \ldots, n)$ are the relative weights on different material phases and V^* is the available material resource. An appropriate choice of w_m allows us to gain control over different material phases either individually or in an integrated manner.

4.2
A note on the numerical examples

Although the material interpolation model proposed in this paper is very general, in the examples presented in this paper, we mainly focus our attention on the three-phase material model. At present, a three-phase material model is more useful than the others because a two-phase material model has been used extensively in the literature and need not be solved again with this new model. The authors also had presented some two-phase material solutions for compliant mechanisms and other problems in their previous work. There does not yet exist a three-phase material design for compliant mechanisms consisting of stiff and flexible materials. Using some of the modern manufacturing methods, three-phase material designs can be fabricated. For instance, shape deposition manufacture (SDM) (Rajagopalan *et al.* 2000) and co-extrusion allow fabrication of a heterogeneous product consisting of stiff and flexible materials. The fabrication of structures consisting of more than three phases is more difficult, but is not impossible. However, the need for such four-phase designs is not yet strongly felt in the application domain.

5
Optimality criteria–based solution procedure

5.1
Solution procedure without material resource (volume) constraint

First, we consider the case where there is no constraint on the total available volume of the material. The first-order necessary condition for the minimum of problem stated in (3) can be obtained as

$$-\frac{\int_{\Gamma_{\mathrm{in}}} F \cdot v \,\mathrm{d}\Gamma}{\left[\int_{\Gamma_{\mathrm{in}}} F \cdot u \,\mathrm{d}\Gamma\right]^2} \epsilon(u) : \frac{\partial E}{\partial \rho} : \epsilon(u) + \frac{\epsilon(v) : \frac{\partial E}{\partial \rho} : \epsilon(u)}{\int_{\Gamma_{\mathrm{in}}} F \cdot u \,\mathrm{d}\Gamma} = 0 \,. \tag{15}$$

The following iterative design variable update scheme is used to meet the above condition:

$$\rho^{(k+1)} = \rho^{(k)} + \frac{\int\limits_{\Gamma_{\text{in}}} F \cdot v \, \mathrm{d}\Gamma}{\left[\int\limits_{\Gamma_{\text{in}}} F \cdot u \, \mathrm{d}\Gamma\right]^2} \epsilon(u) : \frac{\partial E}{\partial \rho} : \epsilon(u) - \frac{\epsilon(v) : \frac{\partial E}{\partial \rho} : \epsilon(u)}{\int\limits_{\Gamma_{\text{in}}} F \cdot u \, \mathrm{d}\Gamma} \tag{16}$$

with limited moving range for $\rho^{(k+1)}$ as shown in (17) where the superscripts $(k+1)$ and (k) denote the k-th and $(k+1)$-st iterations,

$$\rho^{(k)}(1-\xi) \le \rho^{(k+1)} \le \rho^{(k)}(1+\xi)\,. \tag{17}$$

In the following calculations, we use $\xi = \frac{\sigma_1^{(k)}}{5}$.

5.2 Solution procedure with material resource (volume) constraint

For the material interpolation model using peak functions, the material volume constraint can be written as

$$\int\limits_{\Omega} \sum_{m=1}^{n} w_m \exp\left[-\frac{(\rho-\mu_m)^2}{2\sigma_m^2}\right] \mathrm{d}\Omega \le V^*\,. \tag{18}$$

For the optimization problem consisting of equations (3), (4), (5) and (18) and direct calculation method (Yin and Yang 2000a), the necessary condition for the optimum can be obtained as

$$A + \Lambda D = 0\,, \tag{19}$$

where

$$A = -\frac{\int\limits_{\Gamma_{\text{in}}} F \cdot v \, \mathrm{d}\Gamma}{\left[\int\limits_{\Gamma_{\text{in}}} F \cdot u \, \mathrm{d}\Gamma\right]^2} \epsilon(u) : \frac{\partial E}{\partial \rho} : \epsilon(u) + \frac{\epsilon(v) : \frac{\partial E}{\partial \rho} : \epsilon(u)}{\int\limits_{\Gamma_{\text{in}}} F \cdot u \, \mathrm{d}\Gamma}\,,$$

$$D = \sum_{m=1}^{n} -(\rho-\mu_m)/\sigma_m^2 w_m \exp\left[-\frac{(\rho-\mu_m)^2}{2\sigma_m^2}\right]\,,$$

and Λ is the Lagrangian multiplier for the material volume constraint (18). The above optimality condition can be used to derive design variable update formulas in many ways. One of the ways is

$$\rho^{(k+1)} = \rho^{(k)} \left(-\frac{A}{\Lambda D}\right)^q\,, \tag{20}$$

where the value of the exponent q is selected to obtain stable convergence of the scheme. This updating scheme was used by many authors (see, for example Bendsøe and Kikuchi 1988; Yin *et al.* 2000; Yin and Yang 2000a). However, with our present material interpolation we found this updating scheme converges too quickly to get a satisfactory separation between different material phases. For example with three material phases interpolation model, it leads to only two phase material mechanism consisting of either the soft material or the stiff material, and the void. Reducing the value of q helps in slowing the rate of convergence, but it was not sufficient in this problem. An alternate method to overcome this problem is discussed next.

Encouraged by the successful solution of the multiple phase model by the updating scheme proposed for no material resource constraint problem in the last section, we use the following updating scheme for the material volume constraint problem,

$$\rho^{(k+1)} = \rho^{(k)} - \left[A^{(k)} + \Lambda D^{(k)}\right]\,. \tag{21}$$

Then, the Lagrangian multiplier Λ has to be solved using the equation (18). Typically, this equation can be solved by the bisection method (see, for example Bendsøe and Kikuchi 1988). However, the nonlinearity of (18) seems to make it difficult to obtain proper solution here with the move limits as in (17). Therefore, instead of using the exact constraint as in (18), we solve the first-order Taylor series approximation:

$$\int\limits_{\Omega} \sum_{m=1}^{n} w_m \exp\left[-\frac{(\rho^{(k+1)}-\mu_m)^2}{2\sigma_m^2}\right] \mathrm{d}\Omega = \int\limits_{\Omega} B^{(k)} \, \mathrm{d}\Omega + \int\limits_{\Omega} D^{(k)} \left[\rho^{(k+1)} - \rho^{(k)}\right] \mathrm{d}\Omega \le V^*\,, \tag{22}$$

where

$$B = \sum_{m=1}^{n} w_m \exp\left[-\frac{(\rho-\mu_m)^2}{2\sigma_m^2}\right]\,. \tag{23}$$

Using (22), we get analytical expression for Λ with $\overline{V}$ denoting $\int_{\Omega_\ell} D^{(k)}\rho_\ell \, \mathrm{d}\Omega + \int_{\Omega_u} D^{(k)}\rho_u \, \mathrm{d}\Omega$,

$$\Lambda = \frac{V^* - \int\limits_{\Omega} B^{(k)} + D^{(k)}\rho^{(k)} \, \mathrm{d}\Omega - \overline{V}}{\int\limits_{\Omega_a} D^{(k)} D^{(k)} \, \mathrm{d}\Omega}\,. \tag{24}$$

where the domain Ω_ℓ refers to the domain controlled by the lower moving limit, Ω_u to the domain controlled by upper moving limit, and Ω_a to the active domain con-

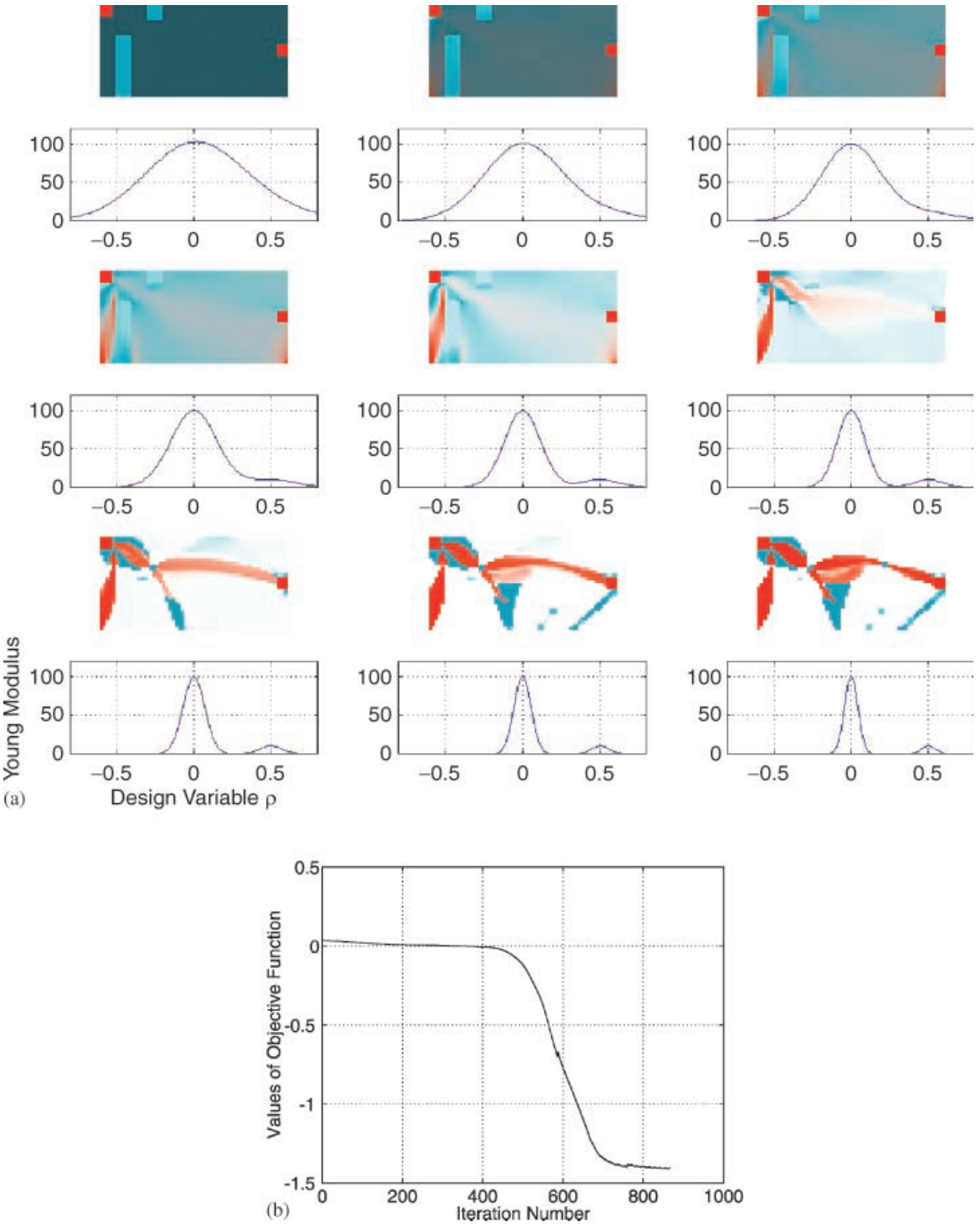

Fig. 5 Example 2. (a) Gradual formation of a three-phase material compliant mechanism with the corresponding material interpolation model (cyan: flexible; red: stiff), (b) convergence history

trolled by equation (18). As is usual in this method, an inner loop is needed to decide these domain partitions (e.g. Bendsøe and Kikuchi 1988; Yin and Yang 2000a). In this inner loop, we find that Ω_a is easily prone to becoming empty. This is because the immediate density domain, which is controlled by (20) or (21), is very small compared with the domain controlled by the upper or lower bounds on the design variables. Very small or completely empty Ω_a poses difficulties during the computation of Λ as is evident from (24). Therefore, we terminate the inner loop before Ω_a becomes very small so that our updating could be continued. This will lead to a minor violation of the constraint during the calculation, which tends to improve when convergence is finally achieved. Example 8 in Sect. 6.4.2 was solved using (22) and (24).

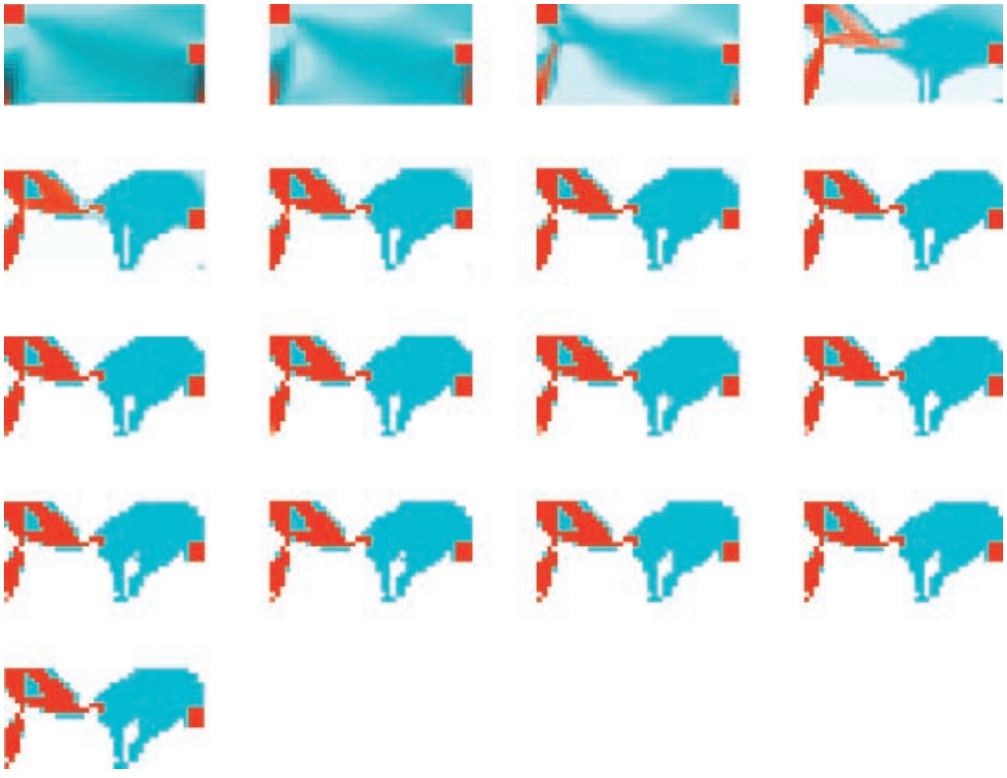

Fig. 6 Example 3: Gradual separation and distribution of a three-phase material compliant mechanism (cyan: flexible; red: stiff)

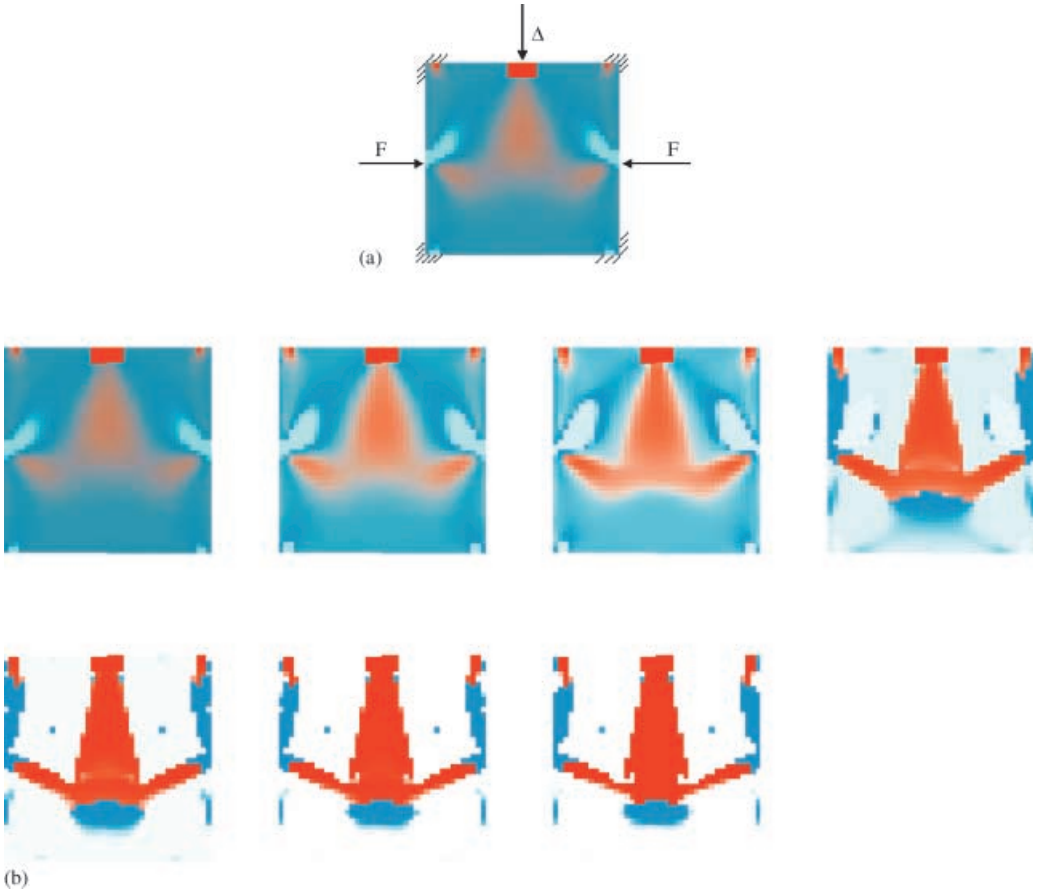

Fig. 7 Example 4: Gradual formation of the mechanism (cyan: flexible; red: stiff). (a) Specification for a three-phase material compliant mechanism, 100 iterations from the uniform initial guess $\rho^{(0)} = 0.4$, (b) formation of the mechanisms as the materials redistribute

6
Numerical examples

6.1
Compliant mechanism design with a two-phase material model

6.1.1
Example 1

The specifications for a compliant mechanism are shown in Fig. 4a. The mechanism is subjected to a vertical force at the upper left corner. The bottom edge of the mechanism is fixed. The output port is located at the middle of the right vertical edge. This point is expected to have a displacement along the direction of 45° downwards. The stiffness of the spring at the output port is $k_s = 0.01E^0$. Young's modulus of the manufacturing material $E = 100E^0$, where E^0 is Young's modulus of a reference material. The domain design with dimension $l \times 2l$ is shown in Fig. 4a. Black area is prescribed as nondesign material area. The grey area is the design area, in which ρ is uniformly distributed for the initial design (e.g. $\rho^{(0)} = 0.1$). Further, the remaining parameters are chosen as $\mu_1 = 0$, and the start value of $2\sigma_1^2 = 0.05$. The value of $2\sigma_1^2 = 0.05$ need not be varied in the two-phase model to get a sensible topology. However, by decreasing it gradually, the intermediate densities can be completely eliminated resulting in a "black and white" or "0-1" design. The final design for this mechanism is shown in Fig. 4b and the convergence history in Fig. 4c. This result is similar to the ones obtained using the SIMP and other two-phase material models.

6.2
Compliant mechanism design with three-phase material model

To optimally juxtapose rigidity and flexibility in compliant mechanisms, we consider the void, a stiff material and a flexible material in our three-phase design examples.

6.2.1
Example 2

The problem specifications for the first example of the three-phase material we present are the same as those for the two-phase material example discussed above. The parameters used in this example include: $2\sigma_1^{(0)2} = 2\sigma_2^{(0)2} = 0.1$, $\mu_1 = 0$, $\mu_2 = 0.5$, $k_s = 0.1E^0$, $E^1 = 10E^2 = 100E^0$, $\omega = 0.005$, $\xi = \sigma_1^{(i)}/5$.

The initial guess for this problem is shown in the first image in Fig. 5a where cyan area denotes the second phase (flexible) material, and the red area the first phase (stiff) material. The solution images are shown in Fig. 5a after every 100 iterations to illustrate how the material distribution takes place. The change of the material model is also shown below each image. The final image in Fig. 5a is the final design. Figure 5b is the convergence history. Although the two materials and void are clearly separated in the final design, some isolated cyan cells remain. This is because during calculation, we uses a special filtering scheme in trying to get the flexural pivot. For the other examples presented next, we do not use this filtering technique.

6.2.2
Example 3

We solved the above example using a different set of parameters: $2\sigma_1^{(0)2} = 2\sigma_2^{(0)2} = 0.05$, $\mu_1 = 0$, $\mu_2 = 0.3$, $k_s = 0.1E^0$, $E^1 = 10E^2 = 100E^0$, $\omega = 0.005$, $\delta = \sigma_1^{(i)}/5$. The initial guess was uniform density of $\rho^{(0)} = 0.35$. The results are shown in Fig. 6. Although the topology is the same as before, the shape and size are substantially different. Nevertheless, both the solutions resemble the topology obtained using the two-phase material model.

6.2.3
Example 4

In this example, the problem specifications are as shown in Fig. 7a where two input forces symmetrically act on the vertical sides of a square design domain. An output displacement is expected at the midpoint of the upper edge of the design domain. The four corners are held fixed. Initial distribution of the material is uniform with $\rho^{(0)} = 0.4$ except a red area at output port where stiff material is prescribed as nondesign area. The material distribution in Fig. 7a is after 100 iterations from the initial guess. The parameters used are as follows: $2\sigma_1^{(0)2} = 0.1$, $2\sigma_2^{(0)2} = 0.2$, $\mu_1 = 0$, $\mu_2 = 0.5$, $k_s = 0.1E^0$, $E^1 = 10E^2 = 100E^0$, $\omega = 0.005$, $\delta = \sigma_1^{(i)}/5$. The results are shown in Fig. 7b.

6.2.4
Example 5

The specifications for the last example of the three-phase design are shown in Fig. 8a. An input force is acting at the upper left corner in the downward direction and an output displacement is expected at a point along the bottom edge towards right. The vertical edge on the right is held fixed and the bottom edge is restrained in the vertical degree of freedom but is free to move in the horizontal direction. Uniform distribution of ρ is used for the initial design. The distribution in the Fig. 8a is after 100 updating calculations. Figure 8b shows the material separation and topology formation. The final image in Fig. 8b is the final design. From the figures, we observe after 800 iterations the distribution of material becomes stable. A clean separation of the two materials and the void can be seen in this example. At the

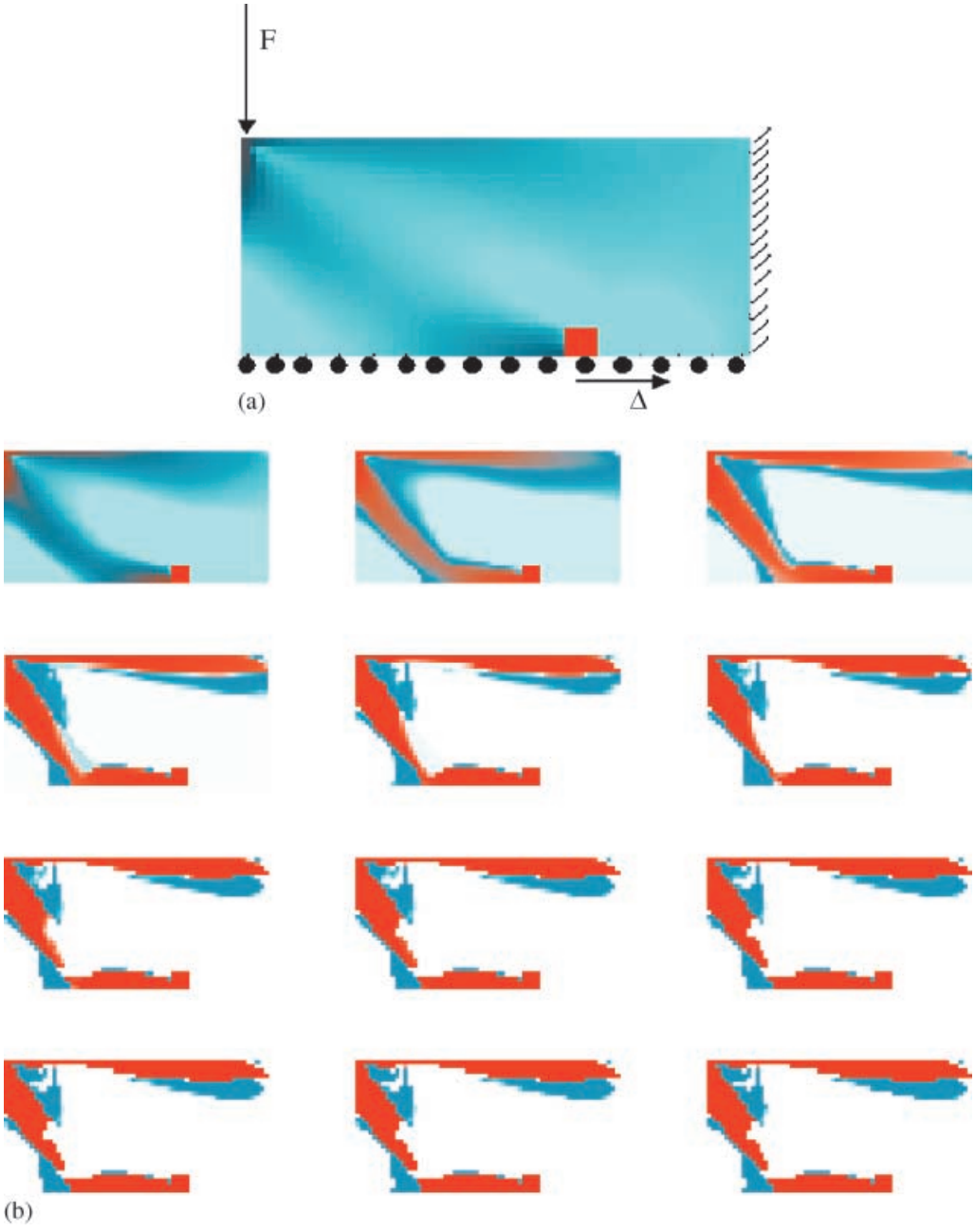

Fig. 8 Example 5: (a) Specification for three-phase material compliant mechanism design, 100 iterations from the uniform initial guess $\rho^{(0)} = 0.4$, (b) gradual formation of the mechanism (cyan: flexible; red: stiff)

lower left corner, the flexible (cyan) material connects the stiff (rigid) material segments indicating a flexural connection.

6.3 Four-phase material compliant mechanism design

6.3.1 Example 6

It is not difficult to get more than three or higher phases of material in a compliant mechanism design. Here, we only give an example up to four-phase material compliant mechanism. The problem specifications are the same as the last example in the Sect. 6.2, but we use a four-phase material model. We use the following parameters in the calculation: $\rho^{(0)} = 0.55$, $2\sigma_1^{(0)2} = 2\sigma_2^{(0)2} = 2\sigma_3^{(0)2} = 0.05$, $\mu_1 = 0$, $\mu_2 = 0.3$, $\mu_3 = 0.5$, $k_s = 0.1E^0$, $E^1 = 2E^2 = 10E^3 = 100E^0$, $\omega = 0.0065$, $\delta = \sigma_1^{(i)}/5$. In Fig. 9, the red area refers to the first phase (stiffest) material, the green the second phase (moderately stiff) material, and the blue the third phase (flexible) material. The first image is after 100 updating calculations from the uniform initial guess and the final image is the converged solution.

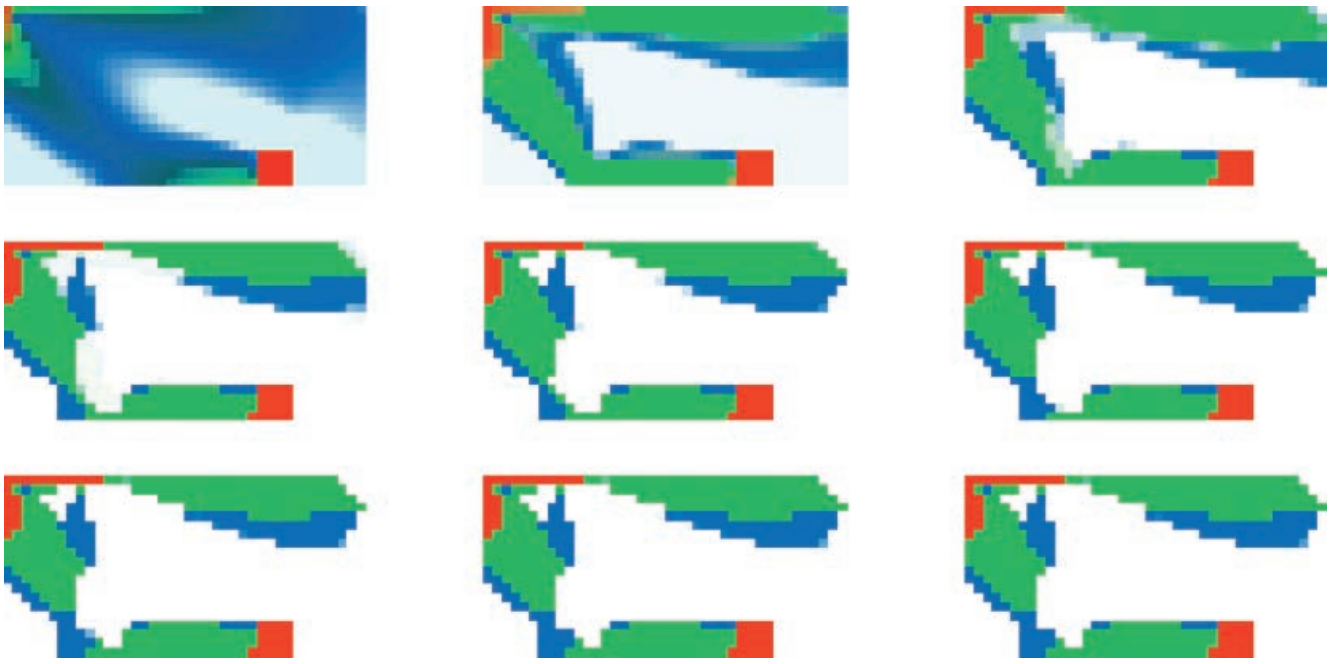

Fig. 9 A four-phase material design for a compliant mechanism (red: very stiff; green: moderately stiff; blue: flexible)

6.4
Two and three-phase material compliant mechanism design with material volume constraint

6.4.1
Example 7

A two-phase material is considered to solve the first example involving a volume constraint. The specifications for this are the same as those for Example 5. The upper bound on the volume, V^*, was 0.4Ω, where Ω is the area of the design domain. The following parameters were used in the numerical calculation: $\rho^{(0)} = 0.4$, $2\sigma_1^{(0)2} = 0.06$, $\mu_1 = 0$, $k_s = 0.1E^0$, $E^1 = 100E^0$, $\omega = 0.008$, $\delta = \sigma_1^{(i)}/5$.

The update scheme in (20) was used to solve this problem. Figure 10a shows the optimal topology, and Fig. 10b shows the iteration history of the objective function and the volume constraint respectively.

6.4.2
Example 8

This example is concerned with the three-phase material compliant mechanism including the material volume constraint. Equal weights were given to the stiff and flexible materials. That is, $w_1 = 1$ and $w_2 = 1$ in (18). The problem specifications are the same as those of Example 5, but we use a three-phase material model and mate-

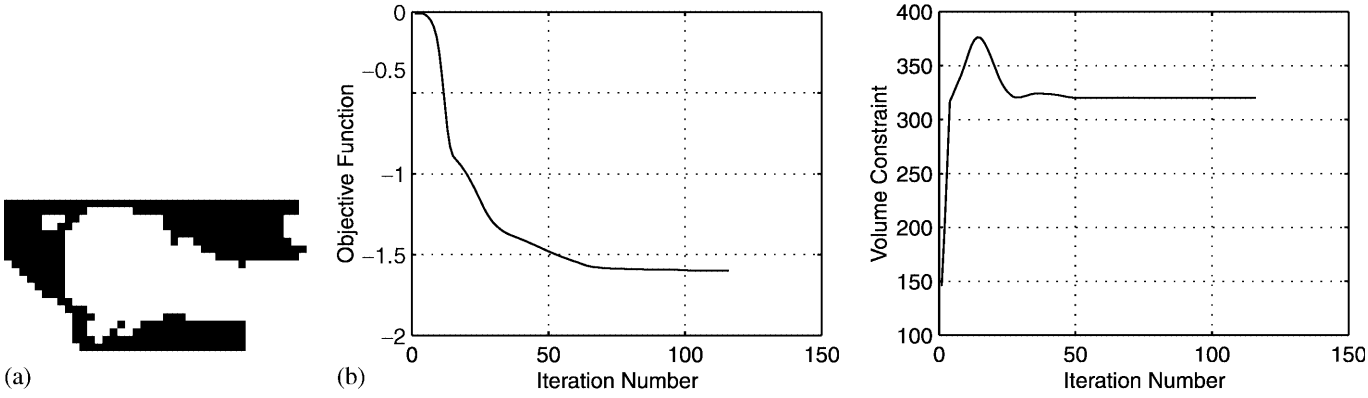

Fig. 10 A two-phase material design for a compliant mechanism with material volume constraint. (a) A two-phase material design for a compliant mechanism with material volume constraint, (b) the convergence history for the material volume constraint and objective function

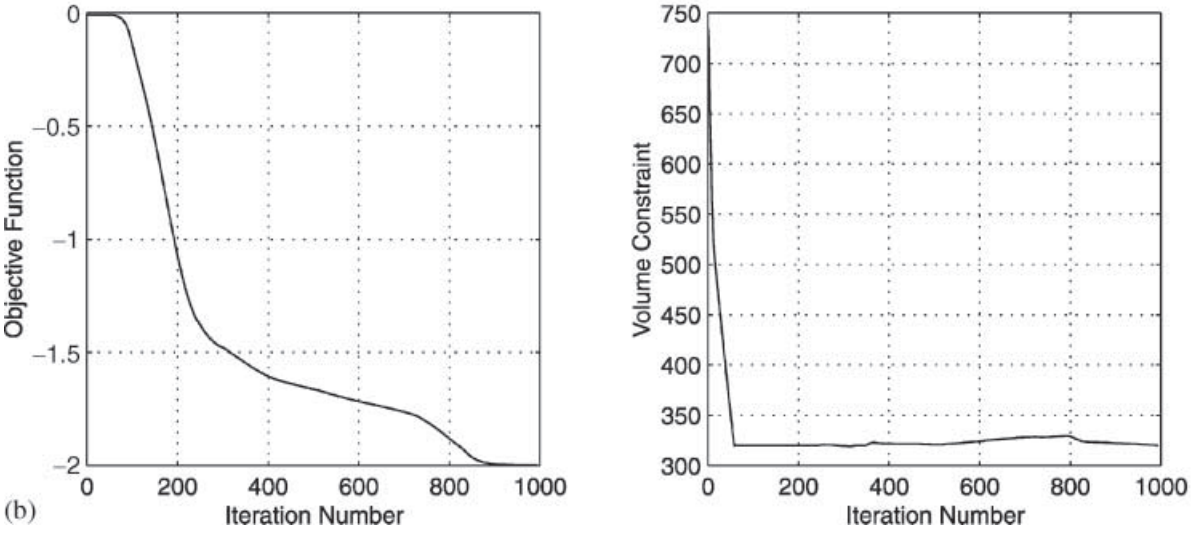

Fig. 11 Example 8. (a) A three-phase material design for a compliant mechanism with material volume constraint (red: very stiff; blue: flexible), (b) the convergence history for the material volume constraint and objective function

rial volume constraint. The parameters used in this calculation were: $\rho^{(0)} = 0.4$, $2\sigma_1^{(0)2} = 2\sigma_2^{(0)2} = 0.06$, $\mu_1 = 0$, $\mu_2 = 0.5$, $k_s = 0.1E^0$, $E^1 = 10E^2 = 100E^0$, $\omega = 0.008$, $\delta = \sigma_1^{(i)}/5$. We prescribed the volume constraint V^* as 0.4Ω, where Ω is the area of the design domain. The update scheme in (21) and (24) was used to solve this problem. In Fig. 11a the red area refers to the first phase (stiff) material, and the blue the third phase (flexible) material. The first image is after 100 iterations from the uniform initial guess and the last image is the converged solution. The convergence histories of the objective function and volume constraint are shown in Fig. 11b. Small violation of the volume constraint can be seen in Fig. 11b. The reason for this was explained in Sect. 5 and was reasoned that this is innocuous.

7 Conclusions

In this paper, we proposed a new material interpolation model, called the *peak function model*, using a linear combination of a normal distribution functions. This model makes it easy to include multiple materials in the design without increasing the design variables. There is considerable flexibility to control the material selection and separation during the optimization process. There is no

need to impose side constraints on the design variables as the model has intrinsic lower and upper bounds on the material property tensor irrespective of the value of the design variable. By gradually adjusting the parameters in the model to create multiple peaks, the final solution can be made to posses pure materials by avoiding intermediate values. Consequently, the need to comply with the existence of physical microstructures that satisfy variational bounds is averted. The material resource constraint can be exercised freely to control the volume of individual phases or the combined heterogeneous structure. Further extensions and the mathematical implications of this new material interpolation model in the topology optimization will be considered in a future publication. Numerous examples solved using this model show that compliant mechanisms consisting of flexible and stiff materials can easily be designed. Thus, this method provides a partial answer to an important question: *for a given problem specification how much compliance is needed and where is it needed in the design domain?* The designs reported in this paper could be manufactured using some of the modern manufacturing techniques that are specifically oriented towards heterogeneous structures.

Acknowledgements The authors are grateful to the National Science Foundation for providing the financial support for this work with a grant # DMR98-00417.

References

Ananthasuresh, G.K.; Kota, S.; Gianchandani, Y. 1994: A methodical approach to the synthesis of Micro-compliant mechanism. *Technical Digest, Solid-State Sensor and actuator Workshop* (held in Hilton Head Island, SC) pp. 189–192

Ananthasuresh, G.K.; Kota, S.; Kikuchi, N. 1994: Strategies for systematic synthesis of compliant MEMS. *Proc. 1994 ASME Winter Annual meeting* (held in Chicago) pp. 677–686

Arfken, D. 1970: Mathematical methods for physicists, New York: Academic Press

Bailey, S.A.; Cham J.G.; Cutkosky, M.R.; Full, R.J. 2000: Biomimetic robotic mechanisms via shape deposition manufacturing. In: Hollerbach, J.; Koditschek, D. (eds.) *Robot Research: 9th Int. Symp.* Berlin, Heidelberg, New York: Springer

Bendsøe, M.P. 1989: Optimal shape design as a material distribution problem. *Struct. Optim.* **1**, 193–202

Bendsøe, M.P. 1995: *Optimization of structural topology, shape, and material*. Berlin, Heidelberg, New York: Springer

Bendsøe, M.P.; Kikuchi, N. 1988: Generating optimal topologies in structural design using a homogenization method. *Comp. Meth. Appl. Mech. Engrg.* **71**, 197–224

Bendsøe, M.P.; Sigmund, O. 2000: Material interpolation schemes in topology optimization. *Danish Center for Applied Mathematics and Mechanics (DCAMM) report*

Frecker, M.; Ananthasuresh, G.K.; Nishiwaki, N.; Kikuchi, N.; Kota, S. 1997: Topological synthesis of compliant mechanisms using multi-criteria optimization. *ASME J. Mech. Des.* **119**, 238–245

Full, R.J. 1997: Invertebrate locomotor systems. In: Dantzler, W. (ed.) *The handbook of comparative physiology*, pp. 853–930. Oxford University Press

Hashin, Z.; Shtrikman, S. 1963: A variational approach to the theory of the elastic behaviour of multiphase materials. *J. Mech. Phys. Solids* **11**, 127–140

Hetrick, J.; Kota, S. 1998: Size and shape optimization of compliant mechanisms. *Proc. ASME Design Engrg. Technical Conf.* (held in Atlanta, GA) Paper #DETC98/ MECH5943

Howell, L.L.; Midha, A. 1996: A loop-closure theory for the analysis and synthesis of compliant mechanisms. *ASME J. Mech. Des.* **118**, 121–125

Ma, Z.-D.; Kikuchi, N. 1995: Topological optimization technique for free vibration problems. *ASME J. Appl. Mech.* **62**, 200–207

Mettlach, G.A.; Midha, A. 1996: Using Burmester theory in the design of compliant mechanisms. *Proc. 1996 ASME Design Engineering Techn. Conf.*, Paper No. 96-DETC/ MECH-1181

Nishiwaki, S.; Frecker, M.; Min, S.; Kikuchi, N. 1998: Topology optimization of compliant mechanisms using the homogenization method. *Int. J. Numer. Meth. Engrg.* **42**, 535–559

Rajagopalan, S.; Goldman, R.; Shin, K-H.; Kumar, V.; Cutkosky, M.; Dutta, D. 2001: Design, processing and freeform-fabrication of heterogeneous objects. (Submitted)

Rozvany, G.I.N.; Bendsøe, M.P.; Kikuchi, N. 1995: Layout optimization of structures. *Appl. Mech. Rev. ASME* **48**, 41–119

Saxena, A.; Kramer, S.N. 1998: A simple and accurate method for determining large deflections in compliant mechanisms subjected to end forces and moments. *ASME J. Mech. Des.* **120**, 392–400

Saxena, A.; Ananthasuresh, G.K. 2000: On an optimality property of compliant topologies. *Struct. Multidisc. Optim.* **19**, 36–49

Sigmund, O. 1994: Materials with prescribed constitutive parameters: an inverse homogenization problem. *Int. J. Solids Struct.* **31**, 2313–2329

Sigmund, O. 1997: On the design of compliant mechanisms using topology optimization. *Mech. Struct. Mach.* **25**, 495–526

Vogel, S. 1995: Better bent than broken. *Discover*, May, 62–67

Yin, L.Z.; Yang, W.; Guo, T.F. 2000: Tunnel reinforcement via topology optimization. *Int. J. Numer. Anal. Meth. Geomech.* **24**, 201–213

Yin, L.Z.; Yang, W. 2000: Topology optimization for tunnel support in layered geological structures. *Int. J. Numer. Meth. Eng.* **47**, 1983–1996

Yin, L.Z.; Yang, W. 2000: Topology optimization to tunnel heaves under different stress biaxialities. *Int. J. Numer. Anal. Meth. Geomech.* **24**, 783–792

Yin, L.Z.; Yang, W. 2001: Minimizing energy flux into a crack tip via topology optimization. (Submitted)

Zhou, M.; Rozvany G.I.N. 1991: The COC algorithm. Part II: topological, geometrical, and generalized shape optimization. *Comp. Meth. Appl. Mech. Engrg.* **89**, 309–336